

# Emergency Collision Avoidance and Mitigation Using Model Predictive Control and Artificial Potential Function

Xu Shang, *Member, IEEE*, Azim Eskandarian, *Senior Member, IEEE*

**Abstract**—Although extensive research in planning has been carried out for normal scenarios, path planning in emergencies has not been thoroughly explored, especially when vehicles move at a higher speed and have less space for avoiding a collision. For emergency collision avoidance, the controller should have the ability to deal with complicated environments and take collision mitigation into consideration since the problem may have no feasible solution. We propose a safety controller by using model predictive control and artificial potential function. A new artificial potential function inspired by line charge is proposed as the cost function for our model predictive controller. The new artificial potential function takes the shape of all objects into consideration. In particular, the artificial potential function that we proposed has the flexibility to fit the shape of the road structures such as the intersection, while the artificial potential function in most of the previous work could only be used in a highway scenario. Moreover, we could realize collision mitigation for a specific part of the vehicle by increasing the quantity of the charge at the corresponding place. We have tested our methods in 192 cases from 8 different scenarios in simulation. The simulation results show that the success rate of the proposed safety controller is 20% higher than using HJ-reachability with system decomposition. It could also decrease 43% of collision that happens at the pre-assigned part.

**Index Terms**—Model Predictive Control, Artificial Potential Function, Collision Avoidance, Crash Mitigation

## I. INTRODUCTION

### A. Background

Almost 3700 people are killed globally every day because of collisions on roads [1]. These collisions could be caused by driver errors, drowsy driving, or driving under influence (DUI). On the other hand, a malfunction in the car, such as a flat tire or brake failure, could also result in collisions. However, these are rare occurrences. Autonomous driving has been considered as a key to solve these problems [2]. It will not have problems of losing concentration like humans and could behave better when other vehicles malfunction and cause an emergency because of its powerful computational speed.

Autonomous driving has been studied for around 40 years and more and more research efforts keep devoting to it recently with the development of computers and sensors. Multiple technologies related to autonomous driving have been already implemented to help people in daily driving such as lane keeping, adaptive cruise control, and automatic parking [3].

100% autonomous driving is expected to be realized in 5-10 years which could significantly improve traffic safety and protect people's lives. However, in some emergencies in which vehicles move at high speeds and there exists less space for maneuvering, even 100% autonomous driving may fail to find a path due to few feasible solutions or even no feasible solution. In this case, collision mitigation becomes extremely important but it lacks sufficient investigations. Based on the fact that the average occupancy of a vehicle is 1.5 people in 2018 [4], our strategy for collision mitigation is to protect the place occupied by passengers and try to redirect the collision to happen at the vehicle's body without passengers.

In this paper, we propose a new safety controller to develop a generalized method to avoid collisions and realize collision mitigation by protecting the pre-assigned part of the vehicle if the collision is inevitable. The overall workflow of our method is shown in Fig. 1. In the rest of this paper, the ego vehicle represents the autonomous vehicle that we could control, while the obstacle vehicle is the vehicle that behaves abnormally and causes an emergency.

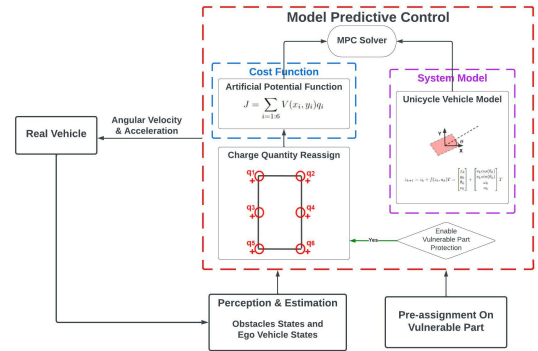


Figure 1. Control Method Workflow

### B. Related Work

Typically, the path planning problem is solved in a hierarchical structure with a high-level behavior planner and a local path planner. The local path planner is supposed to provide a collision-free path while realizing the behavior output from the behavior planner. A lot of work has been done in designing a local path planner for lane-changing behavior when obstacle vehicles approach quickly and occupy the lane for

the ego vehicle. The existing methods include using geometry relationships to design a path and track it [5], implementing model predictive control to change the lane [6], or using machine learning to learn from real drivers' behavior [7]. Local path planners for turning and lane keeping in emergency cases have also been studied. The existing methods include using Bezier curve [8] or choosing paths from pre-defined path libraries [9], [10] and using the probabilistic RRT method [11], [12]. The shortcoming of using this framework is the output command from the behavior planner may have potential conflict with the safety requirement from the local path planner. The local path planner will make a trade-off between realizing the behavior and keeping safe which may lead to a collision in the end. Also, in an emergency, this framework may fail to output multiple behaviors in a short time to avoid collision due to its relatively lower update frequency for the high-level behavior planner.

Constructing safety controllers by using value functions has become more and more popular recently. The core idea of this method in collision avoidance is finding the control invariant set outside the avoid set(obstacle) so that the system will never enter into the avoid set if the control input of the system satisfies the constraints for the control invariant set. HJ-reachability [13] and control barrier function [14] are the state-of-arts in constructing a safety controller. HJ-reachability usually uses the signed distance function between the state and the avoid set as its value function and the optimal control given from it will try to maximize the signed distance at the end of the time period. It could give the largest control invariant set, and deal with system uncertainty and input constraints. The control barrier function usually needs to be hand-crafted by experts or constructed from some machine learning methods [15]. When taking the path planning problem as an optimization problem, both the control barrier function and the modified HJ-reachability would be set as hard constraints to avoid collisions. Some performance terms such as distance to the goal, and energy efficiency could be set as soft constraints to realize specific tasks [14]. However, for HJ-reachability and learning-based control barrier function, they will be computationally expensive for systems with high dimensions. In this case, the system needs to be decomposed to use HJ-reachability which will not guarantee safety for multiple avoid sets [16]. Also, these methods do not consider collision mitigation when the system is not in the control invariant set [17].

There has been only limited research in emergency collision mitigation. Existing methods include testing a series of pre-defined curves and choosing the curve that minimizes the damage [9], [10], constructing the damage severity as a cost function, and solving an optimization problem [18]. The minimum damage is realized by adjusting the relative collision velocity and angle.

In this paper, we try to propose a generalized method to solve emergency collision avoidance problems and minimize the damage by using model predictive control and artificial potential functions. Although the combination of potential functions and model predictive control has been used in several works [19], [20], [21], they have the following limitations:

1. The proposed artificial potential function for road structure only considers the single straight road case and could not be extended in the more complicated environment such as intersection;
2. The proposed artificial potential function does not have the ability to realize collision mitigation;
3. The shape of the obstacle vehicle is considered but the ego vehicle is usually considered as a mass point which limits the use of artificial potential function in multi-vehicle cases. In [22], the shapes of both the obstacle vehicle and the ego vehicle are considered as combinations of several circles. The artificial potential function of the ego vehicle is defined as the maximum value of each individual function among each pair of circles which also doesn't take the ego vehicle as a whole object. Also, as far as we know, in all of the previous work, multi-scenario testing and the analysis of the parameter selection haven't been done thoroughly.

### C. Contributions

The main contributions of our method(APF+MPC) are:1. Proposing a new potential function that takes the shape of obstacle vehicle, ego vehicle, and the road structure into consideration and could be used in multiple scenarios 2. Enabling pre-assignment on vulnerable parts of the vehicle for protection by adjusting the artificial potential function 3. The method can be easily generalized to multi-vehicle scenarios. In this paper, we will try to show the performance of our method in protecting the driver's position as an example. Protection of the other part of the vehicle could be realized in a similar way.

## II. ALGORITHM FRAMEWORK

### A. Problem Statement

Given the trajectory of obstacle vehicles and the fixed location of the road structure, we seek to find a trajectory for the ego vehicle which avoids collisions with both dynamic obstacles(obstacle vehicles) and the static obstacle(road structure). During emergency situations, if the collision is inevitable, we will try to find the trajectory which could protect the pre-assigned part(e.g., driver's position) of the vehicle.

### B. Vehicle and MPC formulation

As shown in Fig. 2, we use the road frame as our reference coordinate in this work.

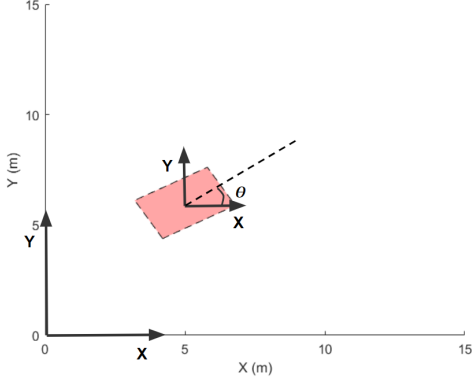


Figure 2. Road Coordinate

The state-space for this system is  $z = [x; y; \theta; v]$  where  $x$  is the longitudinal position,  $y$  is the lateral position,  $\theta$  is the orientation and  $v$  is the speed of the vehicle. The input for this system is  $u = [\omega; a]$  where  $\omega$  and  $a$  are the angular velocity and acceleration of the vehicle. The discrete-time state-space representation of the vehicle could be derived as

$$z_{k+1} = z_k + f(z_k, u_k)T = \begin{bmatrix} x_k \\ y_k \\ \theta_k \\ v_k \end{bmatrix} + \begin{bmatrix} v_k \cos(\theta_k) \\ v_k \sin(\theta_k) \\ \omega_k \\ a_k \end{bmatrix} T, \quad (1)$$

where  $T$  is the discrete time step. Assuming that  $N$  is the prediction horizon, the collision avoidance problem could be formulated as a nonlinear optimization problem:

$$\begin{aligned} \min_{z_k, u_k} \quad & \sum_{k=1}^N J(z_k) \\ \text{s.t.} \quad & z_{k+1} = z_k + f(z_k, u_k)T \\ & u_{\min} \leq u_k \leq u_{\max} \\ & k = 0, \dots, N-1 \end{aligned}$$

$J(z_k)$  represents the potential energy of the system for the state  $z_k$  which is derived using a new artificial potential function. We try to minimize the cost function associated with the potential energy for safe path planning. The dynamic constraints of the vehicle are set as the inequality constraint for MPC in which  $u_{\min}$  and  $u_{\max}$  represent the lower and upper limits of the angular velocity and the acceleration.

### C. Potential Function

We design a new potential function for our problem, and it is inspired by the electrical potential field of line charge. Two basic elements of the potential function are finite-long line charge and infinite-long line charge. The potential function of semi-infinite-long line charge could be derived from them. The potential field of the point  $P$  around the finite-long line charge could be derived as [23]

$$\begin{aligned} V_p &= \int_{-a}^b \frac{k\lambda dx}{r} = \int_{-a}^b \frac{k\lambda dx}{\sqrt{x^2 + d^2}} \\ &= k\lambda \ln \left( \frac{b + \sqrt{b^2 + d^2}}{-a + \sqrt{a^2 + d^2}} \right). \end{aligned} \quad (2)$$

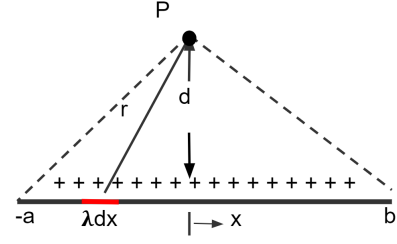


Figure 3. Finite-long line charge

As shown in Fig. 3,  $k$  is the coulomb constant,  $\lambda$  is the line density of the charger,  $a$  is the lower bound of the line,  $b$  is the upper bound of the line and  $d$  is the distance between point  $P$  and the charged finite line. The potential field of the point  $P$  around an infinite-long line charge could be derived as [23]

$$V_p = 2k\lambda \ln\left(\frac{d_0}{d}\right), \quad (3)$$

where  $k$  is the coulomb constant,  $\lambda$  is the line density of the charger,  $d$  is the distance between point  $P$  and the infinite-long line charge and  $d_0$  is the zero potential energy distance which is shown in Fig. 4.

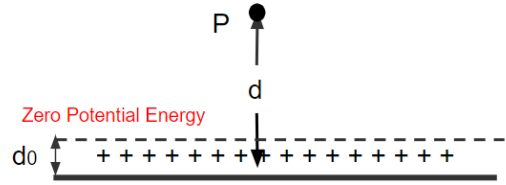


Figure 4. Infinite-long line charge

For the obstacle vehicle, since it is a rectangle in 2D, its potential field is constructed by the superposition of potential fields of four finite-long line charges. The road structure in the highway or the normal road is considered as the infinite-long line charge while it is considered as the semi-infinite-long charge in the intersection. The overall potential field is the superposition of the potential field of all surrounding obstacles. It could be written as  $V = \sum_{i=1:n} w_i V_{Obs_i}$  where  $w_i$  is the weight and  $V_{Obs_i}$  is the potential function of  $i$ th obstacle. The potential fields for highway and intersection with one obstacle vehicle are shown in Fig. 5 and Fig. 6.

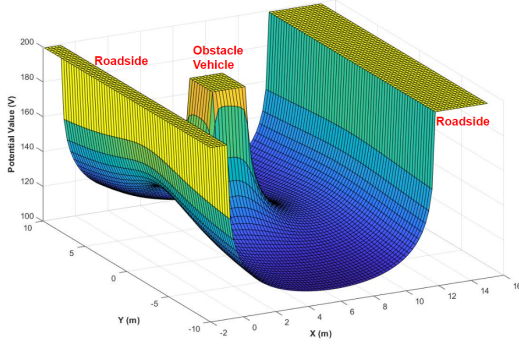


Figure 5. Potential Field in highway

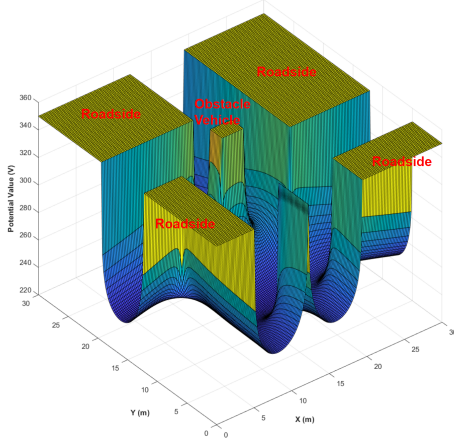


Figure 6. Potential field in intersection

#### D. Potential Energy

Generally, potential energy could be calculated as  $J = Vq$  in which  $V$  represents the potential and  $q$  represents the quantity of the charge. In our method, the potential energy of the system is calculated by placing the charged ego vehicle into the potential field constructed by all the surrounding obstacles. In order to increase the computational speed and realize specific part protection efficiently, we simplify the model of the ego vehicle as 6 point charges, as it is shown in Fig. 7.

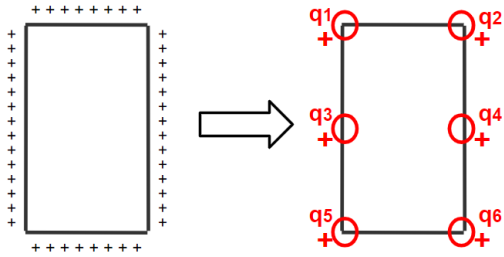


Figure 7. Simplified model for ego vehicle

Then the potential energy of the system could be calculated as

$$J = \sum_{i=1:6} V(x_i, y_i) q_i, \quad (4)$$

where  $(x_i, y_i)$  and  $q_i$  is the position and the charge quantity of the point charge  $i$ . When the driver protection mode is enabled, we will increase the quantity of  $q_1$  to realize driver protection.

#### E. HJ-reachability

In this part, we will introduce system decomposition in HJ-reachability. For basic knowledge of HJ-reachability, please refer to [14].

The total dimension of our system is 8 for one obstacle vehicle and 12 for two obstacle vehicles which are not computationally possible even offline [14]. Thus, we decompose it into two to three subsystems based on the obstacle vehicle's number. We take one obstacle vehicle's case as an example to illustrate the decomposition. We decompose the whole system whose dimension is 8 into subsystem one and subsystem two. Subsystem one is constructed by taking the ego vehicle as the reference and calculating the relative position of the obstacle vehicle and the ego vehicle. This subsystem is used for avoiding collision between the ego vehicle and the obstacle vehicle. The dimension of subsystem one is 6 and the state-space representation of this system is:

$$\dot{z} = \begin{bmatrix} \dot{x}_{rel} \\ \dot{y}_{rel} \\ \dot{\theta}_{Ego} \\ \dot{\theta}_{Obs} \\ \dot{v}_{Ego} \\ \dot{v}_{Obs} \end{bmatrix} + \begin{bmatrix} v_{Obs} \cos(\theta_{Obs}) - v_{Ego} \cos(\theta_{Ego}) \\ v_{Obs} \sin(\theta_{Obs}) - v_{Ego} \sin(\theta_{Ego}) \\ \omega_{Ego} \\ \omega_{Obs} \\ a_{Ego} \\ a_{Obs} \end{bmatrix}. \quad (5)$$

The grid size is  $21 \times 31 \times 11 \times 11 \times 11 \times 11$  uniformly over the 6D system space  $[x_{rel}; y_{rel}; \theta_{Ego}; \theta_{Obs}; v_{Ego}; v_{Obs}] \in [-15, 15] \times [-20, 20] \times [-\pi, \pi] \times [-\pi, \pi] \times [0, 25] \times [0, 25]$ . Subsystem two is used for avoiding collision between the ego vehicle and the road structure and its state-space representation is

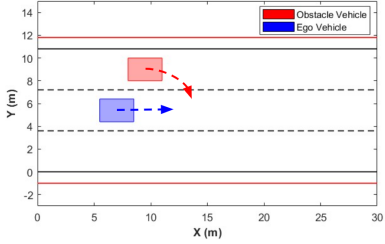
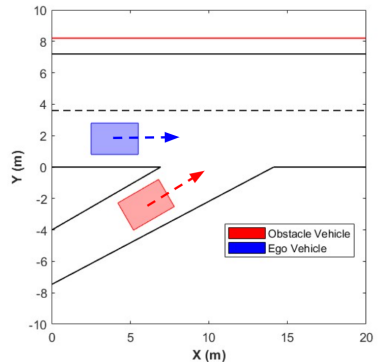
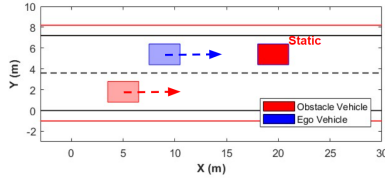
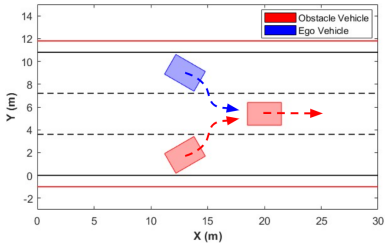
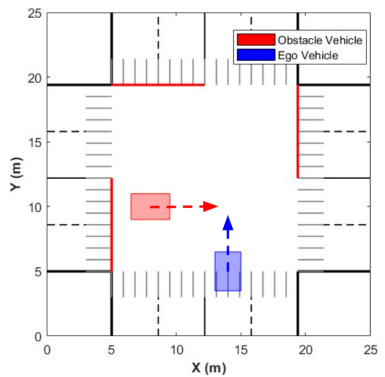
$$\dot{z} = \begin{bmatrix} \dot{x}_{Ego} \\ \dot{y}_{Ego} \\ \dot{\theta}_{Ego} \\ \dot{v}_{Ego} \end{bmatrix} = \begin{bmatrix} v_{Ego} \cos(\theta_{Ego}) \\ v_{Ego} \sin(\theta_{Ego}) \\ \omega_{Ego} \\ a_{Ego} \end{bmatrix}. \quad (6)$$

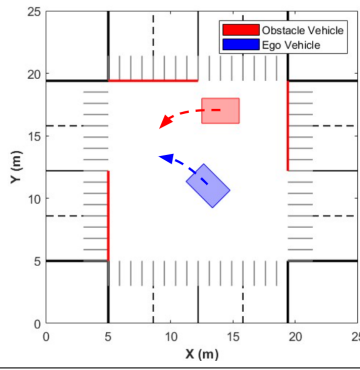
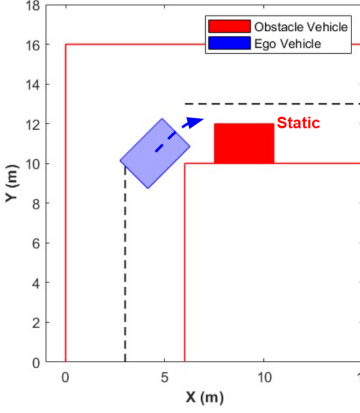
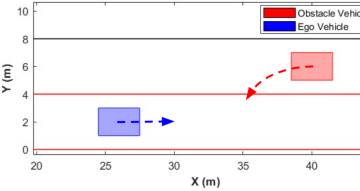
The grid size is  $41 \times 41 \times 21 \times 41$  uniformly over the 4D system space  $[x_{Ego}; y_{Ego}; \theta_{Ego}; v_{Ego}] \in [-5, 25] \times [-5, 25] \times [-\pi, \pi] \times [0, 40]$ . We use the signed distance function as the value function  $V$  for both subsystem one and subsystem two. The value function for the whole system is calculated as  $V = \min\{V_1, V_2\}$  where  $V_1$  and  $V_2$  are value functions of two subsystems and the selection of control input depends on the corresponding subsystem.

### III. SIMULATION RESULTS

We test 192 cases from 8 different scenarios and compare the results of our method with results gotten from HJ-reachability. Scenarios are described in the following table (Table I).

Table I  
SCENARIO DESCRIPTION

Scenario	Ego Vehicle Intention	Obstacle Vehicle Intention	Emergency Casualty
<p><b>Scenario 1:</b></p> <p>It is a three lanes highway scenario with one obstacle vehicle.</p> 	Drive in the middle lane.	Drive in the left lane.	The obstacle vehicle loses control and will keep turning right to the roadside until it gets out of the road.
<p><b>Scenario 2:</b></p> <p>It is a highway merging scenario with one obstacle vehicle.</p> 	Drive in the middle lane.	Merge to the highway from the right lane.	The obstacle vehicle drives too fast or loses control so that it moves across lanes rather than merging into the highway.
<p><b>Scenario 3:</b></p> <p>It is a two lanes highway scenario with two obstacle vehicles.</p> 	Drive in the left lane.	Obstacle vehicle one will stay still in front of the ego vehicle in the left lane and obstacle vehicle two will move at a constant speed in the right lane.	The ego vehicle needs to change to the right lane to avoid collision with obstacle vehicle one while avoiding collision with obstacle vehicle two.
<p><b>Scenario 4:</b></p> <p>It is a three lanes highway scenario with two obstacle vehicles.</p> 	Turn to the middle lane from the left lane and move behind the obstacle vehicle one.	obstacle vehicle one will move at a constant speed in the middle lane and obstacle vehicle two will try to move to the middle lane from the right lane.	Both obstacle vehicle two and ego vehicle plan to turn to the middle lane and occupy the same position behind obstacle vehicle one.
<p><b>Scenario 5:</b></p> <p>It is an intersection scenario with one obstacle vehicle.</p> 	Move straight to pass this intersection from south to north.	Stop and wait for the traffic light to turn green.	The obstacle vehicle breaks the traffic rule and tries to move across the intersection at the red light from west to east. If no action is taken, it will be a severe "T-bone" collision.

Scenario	Ego Vehicle Intention	Obstacle Vehicle Intention	Emergency Casualty
<b>Scenario 6:</b> It is an intersection scenario with one obstacle vehicle. 	Turn left from the south to the west.	Stop and wait for the traffic light to turn green.	The obstacle vehicle breaks the traffic rule and tries to turn left at the red light from east to south. The ego vehicle needs to make the decision to keep turning left or make a U-turn.
<b>Scenario 7:</b> It is a turning scenario in normal road conditions with one obstacle vehicle. 	Turn right.	Stay still.	The ego vehicle suddenly finds a still obstacle vehicle that stays in its lane during the turning because of the blind spot. The ego vehicle needs to realize collision avoidance in a limited space.
<b>Scenario 8:</b> It is a two-lanes heading towards scenario with one obstacle vehicle. 	Drive in the right lane from south to north.	Drive in the left lane from north to south.	The obstacle vehicle loses control which makes it turn left to the ego vehicle's lane.

### A. Results

The results and initial states used in the test are shown in Table II and Fig. 8. In each test, the ego vehicle will start moving from its initial state until distances between the ego vehicle and its surrounding obstacles keep non-decreasing. If no collision happens during this period, we conclude that the ego vehicle successfully avoided the collision.

The average success rate for APF+MPC when protection mode is on is 56.71% and is 57.81% when protection mode is off. Both of them are around 20% higher than the success rate of the HJ-reachability which is 35.94%. From Fig. 8, we could see the success rate by using APF+MPC is also higher than HJ-reachability in each individual scenario except for scenario 4 in which their success rates are the same. Table III and Fig. 9 show the effect of enabling driver protection mode. The average collision rate at the driver's position is 10.94% with protection mode off and 6.24% with protection mode on. Combining looking at Table II and Table III, we could

see enabling the protection mode decrease 43% of collision that happens at the driver's position by decreasing 2% of the success rate which is a little sacrifice.

### B. Case Studies

We totally tested 192 cases and results have been reported in the results section(III. A). To further display the performance of our method, we present the following 4 representative cases. In each case, we compare the performance of our method(APF+MPC) with HJ-reachability and also demonstrate its effectiveness in protecting the vehicle's vulnerable region. As we mentioned in the introduction part(I. C), when the protection mode is on, we would increase the charge quantity at the driver's position. The selection of the charge quantity will be discussed in the discussion part(IV. B).

1) *Case I:* Case I is from scenario 1 and it shows how the ego vehicle will react to a single obstacle vehicle in a highway scenario. In this case, the input of the obstacle vehicle



Table II  
SUCCESS RATE COMPARISON

Scenario	APF + MPC (Protection On)	APF + MPC (Protection Off)	HJ Reachability	Velocity Range(mph)	Initial Relative Position X-Direction(m)	Initial Relative Position Y-Direction(m)
1	50%	41.67%	25%	[45, 80]	3.6	[-2, 4]
2	41.67%	62.5%	20.83%	[45, 80]	4.8	[-4, 2]
3	33%	50%	29.17%	[45, 80]	3.6	[-5, 3]
4	75%	75%	75%	[45, 80]	7.2	[-1, 3]
5	87.5%	70.83%	66.67%	[20, 45]	[-6, -5]	[-5, -3]
6	33%	41.67%	8.33%	[20, 45]	[-3, -1]	[-5, -2]
7	87.75%	75%	33.33%	[20, 55]	[-8, -5]	[-1, 1]
8	45.83%	45.83%	29.17%	[30, 70]	4	[-10, -18]

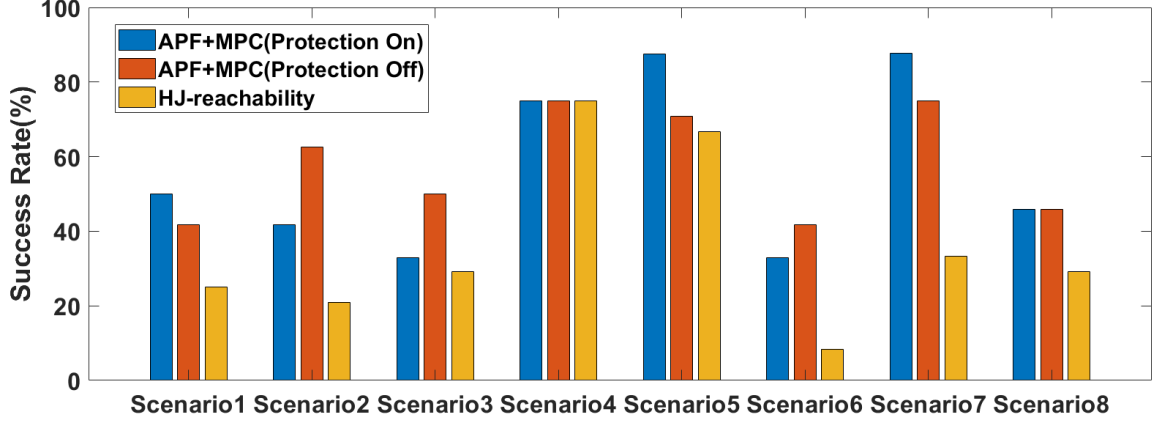


Figure 8. Success rate comparison

Table III  
COLLISION RATE AT DRIVER'S POSITION COMPARISON.

Scenario	APF + MPC (Protection On)	APF + MPC (Protection Off)
1	12.5%	20.83%
2	0%	0%
3	4.17%	25%
4	4.17%	8.33%
5	0%	0%
6	12.5%	12.5%
7	4.17%	0%
8	12.5%	20.83%

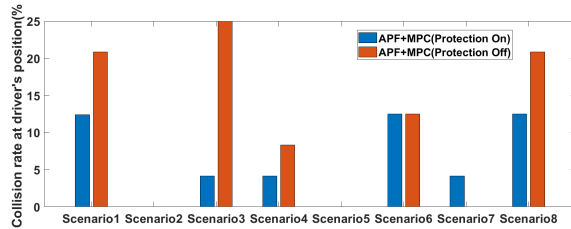


Figure 9. Collision rate at driver's position comparison

is  $[-\pi/2; 3]$ . For the comparison between APF+MPC and HJ-reachability, the initial state of the ego vehicle is  $[7; 5.4; 0; 25]$  while the initial state of the obstacle vehicle is  $[10; 9; 0; 25]$ . For the comparison between protection on and protection off, the initial state of the ego vehicle is  $[8; 5.4; 0; 25]$  while the

initial state of the obstacle vehicle is  $[10; 9; 0; 25]$ . Trajectories of vehicles are shown in Fig. 10, Fig. 11, and Fig. 12. The control inputs are shown in Fig. 13.

**Comparison between APF+MPC&HJ-reachability:** For the APF+MPC method, the ego vehicle will first try to turn right to get some space so that it could decelerate. Then it will turn left to avoid collision with the approaching vehicle. For the HJ-reachability method, the two separate tasks are avoiding collision with the obstacle vehicle and avoiding collision with roadsides. The ego vehicle will turn right in the beginning but it turns too much which makes it lose time to turn left and avoid the collision. It will keep switching between doing these two tasks and the input of the turning rate keeps bumping between the maximum value and the minimum value until the collision happens.

**Comparison between protection on&protection off:** For both protection on and protection off mode, the ego vehicle will turn right and decelerate in the beginning. Then the ego vehicle will turn left and hit the obstacle vehicle. From the input plot Fig. 13, we could see that driver protection is realized by controlling the turning rate. From 0.3s to 0.6s, the ego vehicle will keep turning left when the protection mode is on rather than oscillating when the protection mode is off.

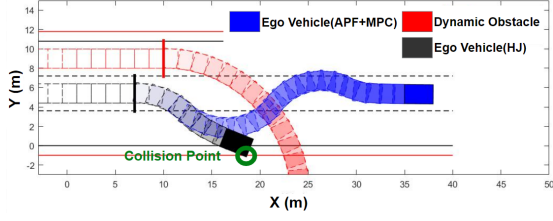


Figure 10. Case I: Comparison between APF+MPC&amp;HJ-reachability

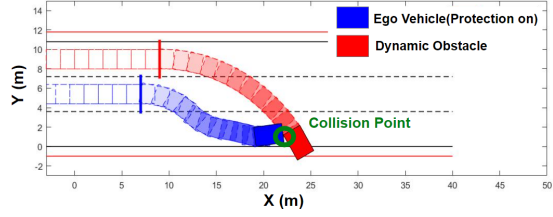


Figure 11. Case I: Protection On

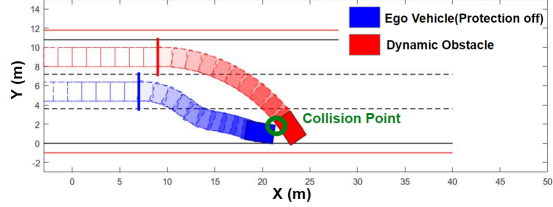


Figure 12. Case I: Protection Off

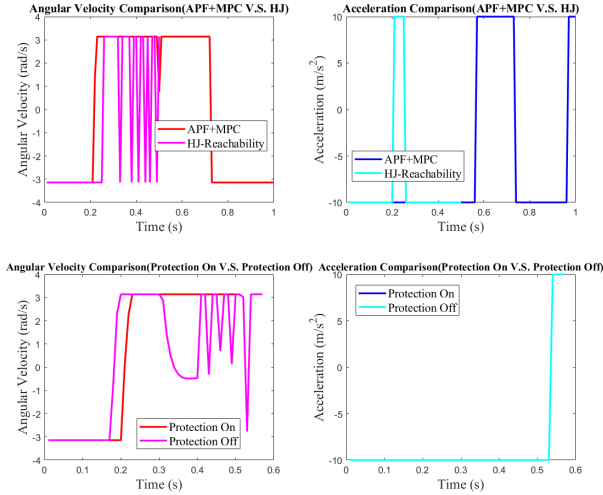


Figure 13. Case I: Control input v.s. Time

2) *Case II*: Case II is from scenario 3 and it shows how the ego vehicle will react to two obstacle vehicles in a highway scenario. In this case, obstacle vehicle one will keep still and obstacle vehicle two will move at a constant speed. For the comparison between APF+MPC and HJ-reachability, the initial state of the ego vehicle is  $[9; 5.4; 0; 20]$  while the initial states for obstacle vehicle one and two are  $[19.5; 5.4; 0; 0]$  and  $[6; 1.8; 0; 30]$ .

For the comparison between protection on and protection off, the initial state of the ego vehicle is  $[4; 5.4; 0; 30]$  while the initial states for obstacle vehicle one and two are  $[19.5; 5.4; 0; 0]$  and  $[6; 1.8; 0; 30]$ . Trajectories of vehicles are shown in Fig. 14, Fig. 15, and Fig. 16. The control inputs are shown in Fig. 17.

**Comparison between APF+MPC&HJ-reachability:** For the APF+MPC method, the ego vehicle will keep accelerating to overtake the obstacle vehicle in the right lane. The ego vehicle will first turn right to avoid the collision with obstacle vehicle one and then turn left to avoid the collision with the roadside. For HJ-reachability, it has three tasks in this case which are avoiding collision with obstacle vehicle one, avoiding collision with obstacle vehicle two, and avoiding collision with the roadside. In the beginning, the priority for the ego vehicle is avoiding obstacle vehicle two in the right lane so it will turn left which makes it lose the opportunity to overtake obstacle vehicle two. The ego vehicle will then keep switching tasks from avoiding collision with obstacle vehicle one at the left lane and the roadside which makes the input of turning rate bump between the maximum value and the minimum value until the collision happens.

**Comparison between protection on&protection off:** For both protection on and protection off mode, the ego vehicle will keep decelerating until it hits obstacle vehicle one in the left lane. From the input plot Fig. 17, we could see the mean difference shows up at 0.2s to 0.35s. During this time period, the ego vehicle will keep turning left when protection mode is on while the ego vehicle will keep turning right when protection mode is off. After 0.35s, the turning rate for both of them keeps bumping. The bumping is caused by the dominant term of the artificial potential function keeps changing.

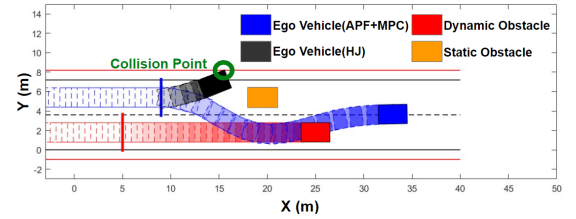


Figure 14. Case II: Comparison between APF+MPC&amp;HJ-reachability

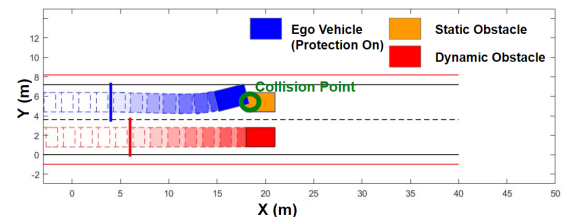


Figure 15. Case II: Protection On

3) *Case III*: Case III is a case from scenario 6 and it shows how the ego vehicle will react to a single obstacle vehicle in the intersection. In this case, the input of the obstacle vehicle is  $[\pi/2; 0]$ . For the comparison between APF+MPC and HJ-reachability, the initial state of the ego vehicle is  $[13; 11;$



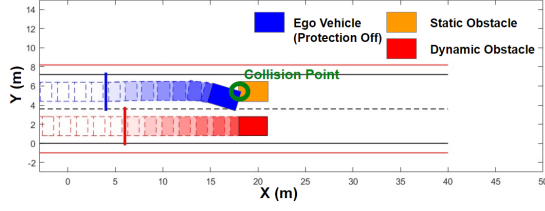


Figure 16. Case II: Protection Off

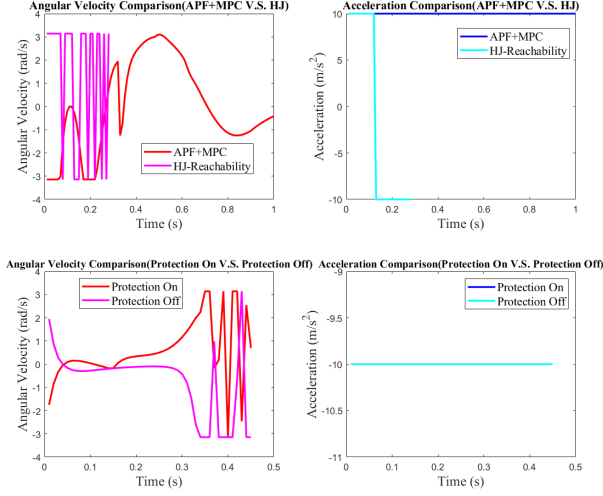


Figure 17. Case II: Control input v.s. Time

0.75 $\pi$ ; 15] while the initial state of the obstacle vehicle is [14; 17;  $\pi$ ; 10]. For the comparison between protection on and protection off, the initial state of the ego vehicle is [13; 11; 0.75 $\pi$ ; 15] while the initial state of the obstacle vehicle is [12; 17;  $\pi$ ; 10]. Trajectories of vehicles are shown in Fig. 18, Fig. 19, and Fig. 20. The control inputs are shown in Fig. 21. **Comparison between APF+MPC&HJ-reachability:** For the APF+MPC method, the ego vehicle will decelerate in the beginning to make a "U" turn and then accelerate to avoid the rear-end collision with the obstacle vehicle. The turning rate keeps at the maximum value which also proves the ego vehicle tends to make a "U" turn. For HJ-reachability, it has two tasks in this case which are avoiding collision with the obstacle vehicle and avoiding collision with the intersection roadside. In the beginning, the priority for the ego vehicle is avoiding the obstacle vehicle so it will turn left. Then the ego vehicle accelerates and tries to overtake the obstacle vehicle. However, the roadside limits the overtaking. The ego vehicle keeps switching tasks and the turning rate keeps bumping which is similar to case I.

**Comparison between protection on&protection off:** For both protection on and protection off mode, the ego vehicle will keep decelerating until it hits the left avoidance area. From the input plot Fig. 21, we could see the mean difference shows up at 0.35s to 0.45s. During this time period, the ego vehicle will keep turning left when protection mode is on while the ego vehicle will keep turning right when protection mode is off.

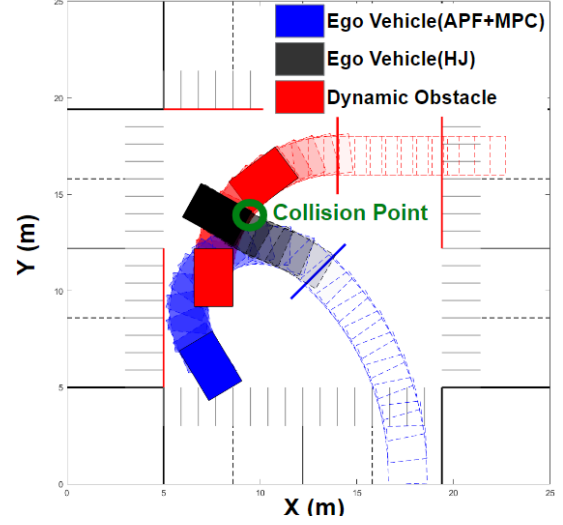


Figure 18. Case III: Comparison between APF+MPC&amp;HJ-reachability

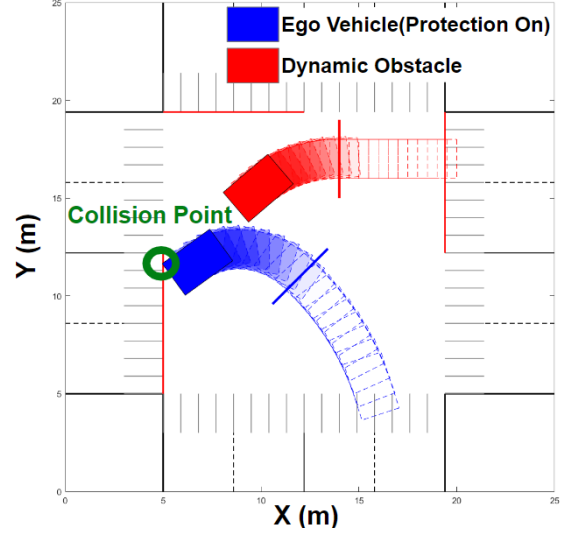


Figure 19. Case III: Protection On

4) *Case IV:* The parameter settings for Case IV are the same as the comparison between protection on&protection off in Case II. The difference is we assume we could also control obstacle vehicle two in Case II. By doing cooperative control, we could avoid an inevitable collision if only controlling a single vehicle.

We define the ego vehicle in the left lane as ego vehicle one and the ego vehicle in the right lane as ego vehicle two. As we could see from Fig. 22 and Fig. 23, in the beginning, ego vehicle two will turn right and keep accelerating to give more space for ego vehicle one. Ego vehicle one will turn right and decelerate to avoid collision with the obstacle vehicle. Then it will accelerate to move away from the obstacle vehicle until it gets close to the ego vehicle two.

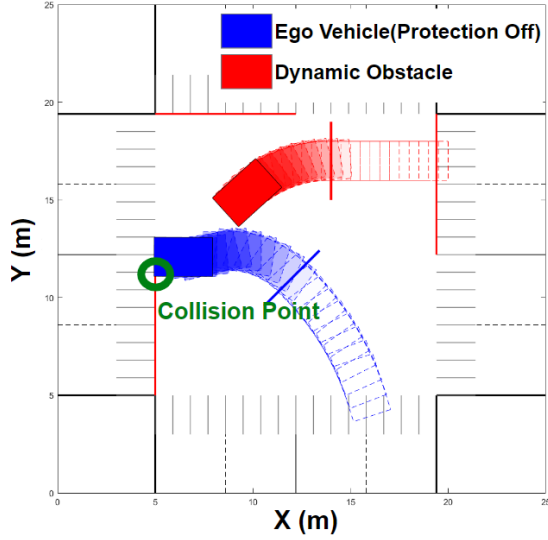


Figure 20. Case III: Protection Off

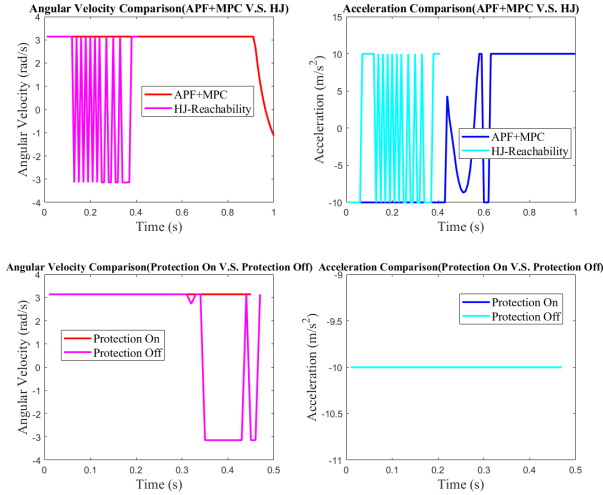


Figure 21. Case III: Control input v.s. Time

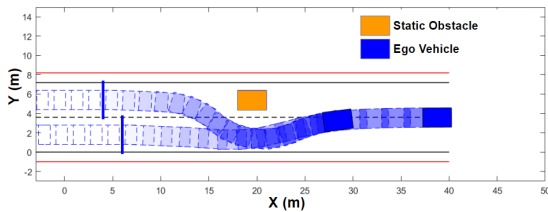


Figure 22. Case IV: Multi-vehicle cooperative control

#### IV. DISCUSSION & FUTURE WORK

##### A. HJ-reachability Revisit

When decomposing the whole system into several subsystems, the problem of sharing control will show up [16]. For each individual subsystem, the control input will always try to make the value function as large as possible which means moving away from the avoid set. Recall that in the algorithm

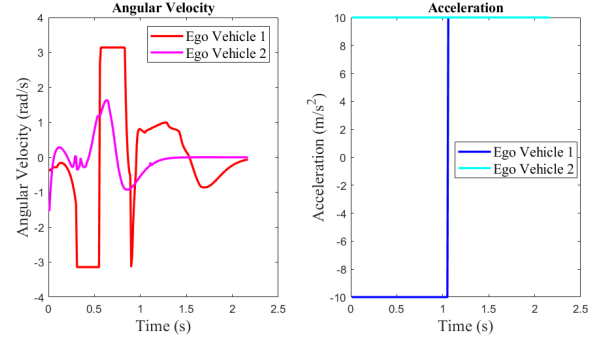


Figure 23. Case IV: Control input v.s. Time

framework part(II. E), we define  $V_1$  and  $V_2$  as value functions of two subsystems. The control input that makes  $V_1$  larger may decrease  $V_2$ . When one of them becomes smaller than zero, a collision will happen. That's the main reason that HJ-reachability will have a lower success rate compared with our method.

Another problem with HJ-reachability is it doesn't consider collision mitigation when the collision is inevitable. We think this problem could be solved by combining the artificial potential function we proposed with HJ-reachability. Rather than directly using the signed-distance function, we could take our new artificial potential function as a reference and change the weight at different positions to realize collision mitigation. Some research has been done in constructing control barrier function by artificial potential function for specific dynamic system [24]. Similar technology could be used for the artificial potential function that we proposed to construct a control barrier function. We could use this control barrier function as the value function in HJ-reachability.

##### B. Parameters Selection

There are two kinds of parameters in our artificial potential function. One is weights between different obstacles and the other is charge quantities for different points in the simplified model in Fig. 7.

The weights for different obstacles will affect the location of the local minimum point in the potential field and thus affect the success rate and the priority for avoiding which obstacle. For the local minimum problem, the use of MPC in our method could partially solve it. The performance will become better as the increasing of prediction horizon while the computational time will also increase. We use the same weight and the same line density  $\lambda$  for all obstacles since we don't assign priority to different obstacles and we want the same length in different obstacles will have the same effect for the ego vehicle.

The charge quantities for different points in the simplified model will make a trade-off between the success rate and the rate of collision at the driver's position. If we increase the charge quantity of the point at the driver's position to an extremely large number, the model will degrade to a point rather than taking the shape of the ego vehicle into consideration. That will avoid most of the collisions happening at the driver's place but decrease the success rate significantly.

To efficiently choose a suboptimal charge quantity in the driver's place, we test 4 different charge quantities at the driver's position which are 1C, 3C, 5C, and 7C. The charge quantities for all the other positions are 1C. As we could see from Fig. 24, 3C is a relatively better choice which has much lower collision rate at the driver's position compared with 1C and a much higher success rate compared with 5C and 7C. Thus, we choose to use 3C at the driver's position when the protection is on.

We also compare the results with our parameter selection with the results from the genetic method with the proposed artificial potential function. The genetic algorithm is inspired by the nature of biological evolution and it has been used for deciding the coefficient of artificial potential function(GA+APF) [25], [26]. The genetic algorithm could also deal with multi-objective optimization so that other factors of the path could be taken into consideration such as smoothness and length. In our case, two objective functions are the maximum potential energy of the whole ego vehicle and the maximum potential energy of the driver's position along the path. We hope to minimize both of them to balance the trade-off problem. However, the algorithm is also required to be implemented in real-time and there isn't enough time to wait for the genetic algorithm to converge. We run the genetic algorithm for 60s in each case to see its performance. The actual time that could be given in a real scenario should be much less than 60s. As we could see from Table IV, compared with APF+MPC(protection on), the collision rate at the driver's position decreases from 6.24% to 1.04% but the success rate also decreases from 56.71% to 48.95%. That shows GA+APF has better driver protection performance but decreases the success rate. Thus, parameter optimization methods run online could not give a Pareto improvement in a limited time.

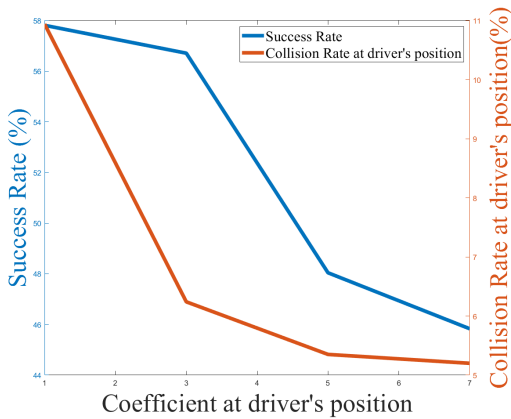


Figure 24. Successful rate and collision rate at driver's position for different driver's position's charge quantities

Reinforcement learning has been used for training the controller based on the classical artificial potential function [27]. In the future, we plan to use a similar method to train our controller offline based on the artificial potential function that we proposed to realize better performance in both driver protection and success rate. We also plan to take different

Table IV  
SUCCESSFUL RATE AND COLLISION RATE AT DRIVER'S POSITION(GA+APF)

Scenario	Success Rate	Collision rate at driver's position
1	54.17%	0%
2	29.17%	0%
3	50%	0%
4	37.5%	4.17%
5	87.5%	0%
6	29.17%	0%
7	58.33%	4.17%
8	45.83%	0%

obstacle types into consideration in more complicated traffic environments and use predicted obstacle trajectories [28].

## V. CONCLUSION

In this paper, we build a safety controller by combining the model predictive control method and artificial potential function for emergency collision avoidance. A new artificial potential function is proposed which is inspired by line charge. There are two main advantages of using this new artificial potential function: 1. It considers the shape of obstacle vehicles, road structures, and the ego vehicle which provides more feasible solutions in an emergency; 2. Specific part collision mitigation could be realized by turning parameters of the artificial potential function. Simulation results in 192 different cases from 8 different scenarios show that our approach works well in different complex scenarios and could be used in multi-vehicle cooperative control. Compared with results from HJ-reachability, the success rate of our approach is 20% higher. Our approach could also decrease 43% of collision in the driver's position with a 2% decrease in the success rate. For the parameters selection problem, we show that the online parameter optimization method(genetic algorithm) which runs in a limited time could not give a Pareto improvement for success rate and collision rate in the driver's position.

## REFERENCES

- [1] "Global road safety," Jun 2022. [Online]. Available: <https://www.cdc.gov/transportationsafety/global/index.html>
- [2] A. Eskandarian, C. Wu, and C. Sun, "Research advances and challenges of autonomous and connected ground vehicles," *IEEE Transactions on Intelligent Transportation Systems*, vol. 22, no. 2, pp. 683–711, 2019.
- [3] A. Eskandarian, *Handbook of intelligent vehicles*. Springer, 2012, vol. 2.
- [4] S. C. Davis and R. G. Boundy, "Transportation energy data book: Edition 39," Oak Ridge National Lab.(ORNL), Oak Ridge, TN (United States), Tech. Rep., 2021.
- [5] Q. Cui, R. Ding, C. Wei, and B. Zhou, "A hierarchical framework of emergency collision avoidance amid surrounding vehicles in highway driving," *Control Engineering Practice*, vol. 109, p. 104751, 2021.
- [6] C. Choi, Y. Kang, and S. Lee, "Emergency collision avoidance maneuver based on nonlinear model predictive control," in *2012 IEEE International Conference on Vehicular Electronics and Safety (ICVES 2012)*. IEEE, 2012, pp. 393–398.
- [7] S. Cong, W. Wang, J. Liang, L. Chen, and Y. Cai, "An automatic vehicle avoidance control model for dangerous lane-changing behavior," *IEEE Transactions on Intelligent Transportation Systems*, 2021.
- [8] V. Khattar and A. Eskandarian, "Reactive online motion re-planning for crash mitigation in autonomous vehicles using bezier curve optimization," in *ASME International Mechanical Engineering Congress and Exposition*, vol. 84553. American Society of Mechanical Engineers, 2020, p. V07BT07A016.

- [9] C. Sun and A. Eskandarian, "A predictive frontal and oblique collision mitigation system for autonomous vehicles," *ASME Letters in Dynamic Systems and Control*, vol. 1, no. 4, 2021.
- [10] J. Wei, J. M. Snider, T. Gu, J. M. Dolan, and B. Litkouhi, "A behavioral planning framework for autonomous driving," in *2014 IEEE Intelligent Vehicles Symposium Proceedings*. IEEE, 2014, pp. 458–464.
- [11] X. Wu, A. Nayak, and A. Eskandarian, "Motion planning of autonomous vehicles under dynamic traffic environment in intersections using probabilistic rapidly exploring random tree," *SAE International Journal of Connected and Automated Vehicles*, vol. 4, no. 12-04-04-0029, 2021.
- [12] W. Xihui *et al.*, "Predictive motion planning of vehicles at intersection using a new gpr and rrt," in *2020 IEEE 23rd International Conference on Intelligent Transportation Systems (ITSC)*. IEEE, 2020, pp. 1–6.
- [13] S. Bansal, M. Chen, S. Herbert, and C. J. Tomlin, "Hamilton-jacobi reachability: A brief overview and recent advances," in *2017 IEEE 56th Annual Conference on Decision and Control (CDC)*. IEEE, 2017, pp. 2242–2253.
- [14] A. D. Ames, X. Xu, J. W. Grizzle, and P. Tabuada, "Control barrier function based quadratic programs for safety critical systems," *IEEE Transactions on Automatic Control*, vol. 62, no. 8, pp. 3861–3876, 2016.
- [15] M. Srinivasan, A. Dabholkar, S. Coogan, and P. A. Vela, "Synthesis of control barrier functions using a supervised machine learning approach," in *2020 IEEE/RSJ International Conference on Intelligent Robots and Systems (IROS)*. IEEE, 2020, pp. 7139–7145.
- [16] M. Chen, S. L. Herbert, M. S. Vashishtha, S. Bansal, and C. J. Tomlin, "Decomposition of reachable sets and tubes for a class of nonlinear systems," *IEEE Transactions on Automatic Control*, vol. 63, no. 11, pp. 3675–3688, 2018.
- [17] K. Leung, E. Schmerling, M. Zhang, M. Chen, J. Talbot, J. C. Gerdes, and M. Pavone, "On infusing reachability-based safety assurance within planning frameworks for human–robot vehicle interactions," *The International Journal of Robotics Research*, vol. 39, no. 10-11, pp. 1326–1345, 2020.
- [18] H. Wang, Y. Huang, A. Khajepour, Y. Zhang, Y. Rasekhipour, and D. Cao, "Crash mitigation in motion planning for autonomous vehicles," *IEEE transactions on intelligent transportation systems*, vol. 20, no. 9, pp. 3313–3323, 2019.
- [19] Z. Huang, Q. Wu, J. Ma, and S. Fan, "An apf and mpc combined collaborative driving controller using vehicular communication technologies," *Chaos, Solitons & Fractals*, vol. 89, pp. 232–242, 2016.
- [20] J. Ji, A. Khajepour, W. W. Melek, and Y. Huang, "Path planning and tracking for vehicle collision avoidance based on model predictive control with multiconstraints," *IEEE Transactions on Vehicular Technology*, vol. 66, no. 2, pp. 952–964, 2016.
- [21] C. Liu, S. Lee, S. Varnhagen, and H. E. Tseng, "Path planning for autonomous vehicles using model predictive control," in *2017 IEEE Intelligent Vehicles Symposium (IV)*. IEEE, 2017, pp. 174–179.
- [22] M. Cao, R. Wang, J. Wang, and N. Chen, "An integrated mpc approach for fwia autonomous ground vehicles with emergency collision avoidance," in *2018 21st International Conference on Intelligent Transportation Systems (ITSC)*. IEEE, 2018, pp. 2432–2437.
- [23] "Electric field of line charge." [Online]. Available: <http://hyperphysics.phy-astr.gsu.edu/hbase/electric/elelin.html>
- [24] A. Singletary, K. Klingebiel, J. Bourne, A. Browning, P. Tokumaru, and A. Ames, "Comparative analysis of control barrier functions and artificial potential fields for obstacle avoidance," in *2021 IEEE/RSJ International Conference on Intelligent Robots and Systems (IROS)*. IEEE, 2021, pp. 8129–8136.
- [25] P. Vadakkepat, K. C. Tan, and W. Ming-Liang, "Evolutionary artificial potential fields and their application in real time robot path planning," in *Proceedings of the 2000 congress on evolutionary computation. CEC00 (Cat. No. 00TH8512)*, vol. 1. IEEE, 2000, pp. 256–263.
- [26] X. Xu, J. Xie, and K. Xie, "Path planning and obstacle-avoidance for soccer robot based on artificial potential field and genetic algorithm," in *2006 6th World Congress on Intelligent Control and Automation*, vol. 1. IEEE, 2006, pp. 3494–3498.
- [27] Q. Yao, Z. Zheng, L. Qi, H. Yuan, X. Guo, M. Zhao, Z. Liu, and T. Yang, "Path planning method with improved artificial potential field—a reinforcement learning perspective," *IEEE Access*, vol. 8, pp. 135 513–135 523, 2020.
- [28] A. Nayak, A. Eskandarian, and Z. Doerzaph, "Uncertainty estimation of pedestrian future trajectory using bayesian approximation," *arXiv preprint arXiv:2205.01887*, 2022.



**Xu Shang** received the B.S. degree in mechanical engineering from Shanghai Jiao Tong university and the M.S. degree from University of Michigan. He is currently pursuing the Ph.D. degree in mechanical engineering from Virginia Tech. His current research interests include robotics and control, decision making, path planning, and connected vehicles.



**Azim Eskandarian** received the B.S. and D.Sc. degrees from George Washington University (GWU) and the M.S. degree from Virginia Tech all in mechanical engineering. He was a Professor of engineering and applied science with GWU and the Founding Director of the Center for Intelligent Systems Research from 1996 to 2015. From 2002 to 2015, he was the Director of the Transportation Safety and Security University Area of Excellence. In 1992, he was a Co-Founder of the National Crash Analysis Center. From 1998 to 2002 and 2013 to 2015, he was the Director of the National Crash Analysis Center. He was an Assistant Professor with Pennsylvania State University, York, PA, USA, from 1989 to 1992, and an Engineer/Project Manager in industry from 1983 to 1989. He has been a Professor and the Head of the Mechanical Engineering Department with Virginia Tech (VT), since 2015. In 2018, he became the Nicholas and Rebecca Des Champs Chaired Professor. He established the Autonomous Systems and Intelligent Machines Laboratory at VT to conduct research on intelligent and autonomous vehicles and mobile robots. He is a fellow of ASME and a member of SAE professional societies. He received the IEEE ITS Society's Outstanding Researcher Award in 2017 and GWU's School of Engineering Outstanding Researcher Award in 2013.